Field-induced magnetic transitions in the quasi-two-dimensional heavy-fermion antiferromagnets Ce_nRhIn_{3n+2} ($n=1$ or 2)

A. L. Cornelius
Department of Physics, University of Nevada, Las Vegas, Nevada 89154-4002

P. G. Pagliuso, M. F. Hundley, and J. L. Sarrao
Materials Science and Technology Division, Los Alamos National Laboratory, Los Alamos, New Mexico 87545
(Received 18 April 2001; published 18 September 2001)

We have measured the field-dependent heat capacity in the tetragonal antiferromagnets $CeRhIn_5$ and Ce_2RhIn_8, both of which have an enhanced value of the electronic specific heat coefficient $\gamma \sim 400$ mJ/mol Ce K^2 above T_N. For $T<T_N$, the specific heat data at zero applied magnetic field are consistent with the existence of an anisotropic spin-density wave opening a gap in the Fermi surface for $CeRhIn_5$, while Ce_2RhIn_8 shows behavior consistent with a simple antiferromagnetic magnon. From these results, the magnetic structure, in a manner similar to the crystal structure, appears more two dimensional in $CeRhIn_5$ than in Ce_2RhIn_8 where only about 12% of the Fermi surface remains ungapped relative to 92% for Ce_2RhIn_8. When $B||c$, both compounds behave in a manner expected for heavy-fermion systems as both T_N and the electronic heat capacity decrease as field is applied. When the field is applied in the tetragonal basal plane ($B||a$), $CeRhIn_5$ and Ce_2RhIn_8 have very similar phase diagrams which contain both first- and second-order field-induced magnetic transitions.

DOI: 10.1103/PhysRevB.64.144411 PACS number(s): 71.18.+y, 71.27.+a, 75.30.Kz, 65.40.−b

I. INTRODUCTION

Ce_nRhIn_{2n+3} ($n=1$ or 2) crystallize in the quasi-two-dimensional (quasi-2D) tetragonal structures Ho_nCoGa_{2n+3}, and both are moderately heavy-fermion antiferromagnets ($\gamma \sim 400$ mJ/mol Ce K^2 for both systems above $T_N=3.8$ K for $n=1$ and 2.8 K for $n=2$). The evolution of the ground states of $CeRhIn_5$ as a function of applied pressure, including a pressure-induced first-order superconducting transition at 2.1 K, is unlike any previously studied heavy-fermion system and is attributed to the quasi-2D crystal structure.[1] In a similar manner to $CeRhIn_5$, T_N is seen to change only slightly with pressure and abruptly disappear in Ce_2RhIn_8, though superconductivity has not yet been observed.[2]

A previous zero-field heat capacity study on $CeRhIn_5$ revealed that the anisotropic crystal structure leads to a quasi-2D electronic and magnetic structure.[4] We have performed measurements of the heat capacity in applied magnetic fields for $CeRhIn_5$ and Ce_2RhIn_8 in an attempt to further understand the electronic and magnetic properties of these compounds. We find that for magnetic fields applied along the tetragonal c axis, both systems behave like typical heavy-fermion compounds[5] as both T_N and γ_0 decrease as field is increased. Very different behavior is seen when the field is directed along the a axis as T_N is found to increase and numerous field-induced transitions, both of first and second order, are observed. These transitions correspond to magnetic field-induced changes in the magnetic structure. In agreement with what one might expect, the magnetic properties seem less 2D as the crystal structure becomes less 2D going from single-layer $CeRhIn_5$ to double layer Ce_2RhIn_8 (note that as $n\rightarrow\infty$, one gets the 3D cubic system $CeIn_3$).

II. RESULTS

Single crystals of Ce_nRhIn_{2n+3} were grown using a flux technique described elsewhere.[6] The residual resistivity ratio between 2 and 300 K using a standard four-probe measurement and was found to be greater than 100 for all measured crystals, indicative of high-quality samples. A clear kink was observed in the resistivity at $T_N=3.8$ K for $CeRhIn_5$ and $T_N=2.8$ K in Ce_2RhIn_8. The polycrystalline average of the high-temperature ($T>200$ K) anisotropic susceptibility gives effective magnetic moments very near the expected value of $2.54\mu_B$/Ce for the full moment of $J=5/2$ Ce. The anisotropy in the magnetization is larger for $CeRhIn_5$ relative to Ce_2RhIn_8 with the overall susceptibility being fit by three crystal-field doublets.[2,3] The specific heat was measured on a small (~ 10 mg) sample employing a standard thermal relaxation method.

The single crystals were typically rods with dimensions from 0.1 to 10 mm with the long axis of the rod found to be along the $\langle 100\rangle$ axis of the tetragonal crystal. The samples were found to crystallize in the primitive tetragonal Ho_nCoGa_{2n+3}-type structure[7,8] with lattice parameters of $a=0.4652(1)$ nm and $c=0.7542(1)$ nm for $n=1$ and $a=0.4665(1)$ nm and $c=1.2244(5)$ nm for $n=2$.[1,2] The crystal structure of Ce_nRhIn_{2n+3} can be viewed as $(CeIn_3)_n(RhIn_2)$ with alternating n cubic ($CeIn_3$) and one ($RhIn_2$) layers stacked along the c axis. By looking at the crystal structure, we would expect that antiferromagnetic (AF) correlations will develop in the ($CeIn_3$) layers in a manner similar to bulk $CeIn_3$.[9] The AF ($CeIn_3$) layers will then be weakly coupled by an interlayer exchange interaction through the ($RhIn_2$) layers which leads to a quasi-2D magnetic structure. This has been shown to be true as the moments are AF ordered within the tetragonal basal a plane but display a modulation along the c axis which is incommensurate with the lattice for $CeRhIn_5$.[10] As n is increased, the crystal structure should become more 3D ($n=\infty$ being the 3D cubic system $CeIn_3$) and the effects of the interlayer

 ©2001 The American Physical Society

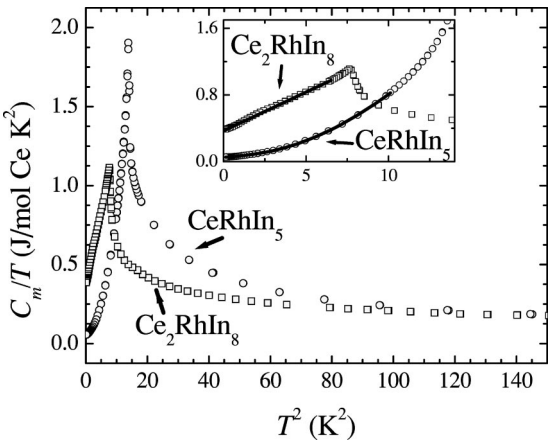

FIG. 1. The zero-field magnetic specific heat C_m divided by temperature T vs T^2 for $CeRhIn_5$ and Ce_2RhIn_8. The inset displays the range $T^2<15$ K^2 corresponding to temperatures below T_N. The lines are fits described in the text.

coupling should become less important, causing the magnetic and electronic structure to be more 3D. Indeed, the magnetic structure in Ce_2RhIn_8 does not display an incommensurate spin-density wave (SDW).[11]

The zero-field data from specific heat measurements are shown in Fig. 1. A peak at T_N is clearly seen for both samples, indicating the onset of magnetic order. The entropy associated with the magnetic transition is $\sim 0.3R \ln 2$ with the remaining $0.7R \ln 2$ recovered by 20 K for both $n=1$ and 2. For $T>T_N$ the data could not be fit by simply using $C/T=\gamma+\beta_l T^2$, where γ is the electronic specific heat coefficient and β_l is the lattice Debye term. As found previously, one needs to use isostructural, nonmagnetic La_nRhIn_{2n+3} to subtract the lattice contribution to C.[1] After subtracting the lattice contribution, it is still difficult to extract a value of γ from the data. However, by performing a simple entropy balance construction, a value of $\gamma \approx 400$ mJ/mol Ce K^2 is found for both $n=1$ and 2.

For temperatures below T_N, as found before on $CeRhIn_5$,[4] the magnetic heat capacity data, where the corresponding La compound is used to subtract the lattice contribution, can be fit using the equation

$$C_m/T=\gamma_0+\beta_M T^2+\beta'_M(e^{-E_g/k_B T})T^2, \qquad (1)$$

where γ_0 is the zero-temperature electronic term, $\beta_M T^2$ is the standard AF magnon term, and the last term is an activated AF magnon term. The need for an activated term to describe heat capacity data has been seen before in other Ce and U compounds,[4,12–14] and the term rises from an AF SDW with a gap in the excitation spectrum due to anisotropy. This is consistent with Fermi surface measurements which show a gap in the electronic structure.[4] As discussed previously, the $CeRhIn_5$ magnetic structure indeed displays an anisotropic SDW with modulation vector (1/2,1/3,0.297),[10] which is consistent with this picture. Since there is a well-defined magnetic moment at high temperatures, the magnetically ordered SDW state is likely influenced by the existence of Fermi surface nesting effects. The inset to Fig. 1 shows the data for

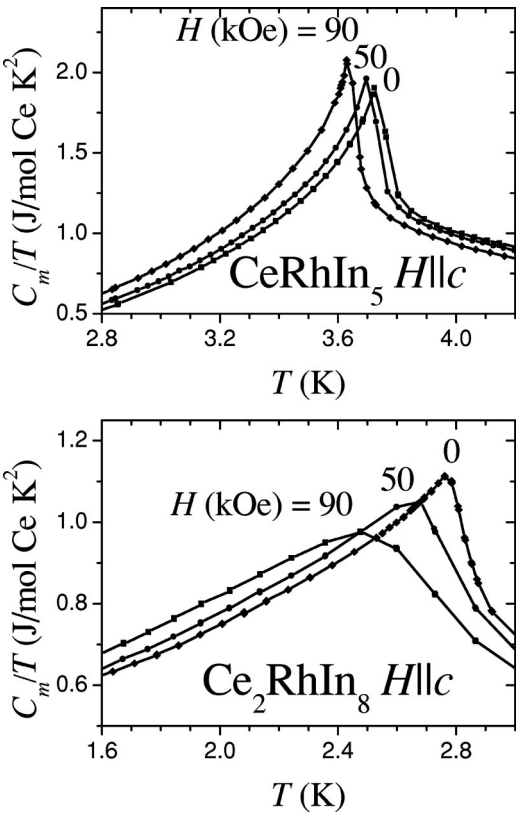

FIG. 2. The magnetic specific heat C_m divided by temperature T vs T for $CeRhIn_5$ (top) and Ce_2RhIn_8 (bottom) in various applied fields applied along the c axis.

$T<T_N$ and the lines are fits to Eq. (1) for $T^2<(0.85T_N)^2$. We find that the activated term is *not* necessary to fit the Ce_2RhIn_8 data. Rather, there appears to be a small feature in the heat capacity centered around ~ 1.5 K whose origin is unknown. This feature is also observed in transport measurements and is known to persist as a function of pressure.[15] A summary of the fit parameters, along with data on $CeIn_3$,[16] is given in Table I. These results lead us to the conclusion that the magnetically ordered state in $CeRhIn_5$ consists of an anisotropic SDW that opens up a gap on the order of 8 K in the Fermi surface, while no such gap is seen in Ce_2RhIn_8, consistent with its commensurate structure. Note that the values for $CeRhIn_5$ are slightly different from a previous report where the lattice contribution from $LaRhIn_5$ was not subtracted from the raw data.[4] From the ratio of the electronic contribution for temperatures above and below T_N, we esti-

TABLE I. Calculated zero-field heat capacity fit parameters for Ce_nRhIn_{2n+3}. Data for $CeIn_3$ are taken from Ref. 16. The various parameters are defined in the text. Units for γ_0 and γ are mJ/mol Ce K^2 and for β_M and β'_M are mJ/mol Ce K^4.

	n	T_N (K)	γ_0	γ	β_M	β'_M	E_g/k_B (K)
$CeRhIn_5$	1	3.72	56	400	24.1	706	8.2
Ce_2RhIn_8	2	2.77	370	400	93.2	-	-
$CeIn_3$	∞	10	136	144	15	-	-

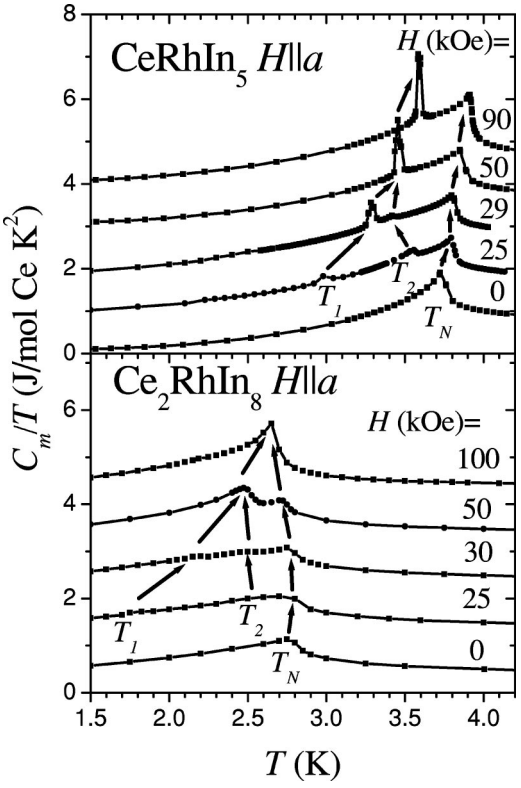

FIG. 3. The magnetic specific heat C_m divided by temperature T vs T for $CeRhIn_5$ (top) and Ce_2RhIn_8 (bottom) in various applied fields applied along the a axis. T_N corresponds to the antiferromagnetic ordering temperature, and T_1 and T_2 correspond to field-induced first- and second-order transitions, respectively. The curves are offset by 1 J/mol Ce K^2 for each successive curve.

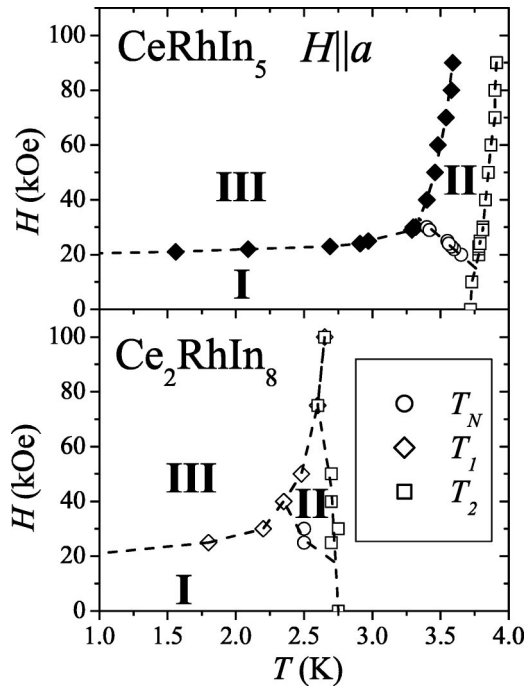

FIG. 4. The cumulative phase diagrams for $CeRhIn_5$ and Ce_2RhIn_8 for various applied fields applied along the a axis. T_N corresponds to the antiferromagnetic ordering temperature, and T_1 and T_2 correspond to field-induced transitions as discussed in text (open symbols are second-order transitions and solid symbols are first-order transitions). The dashed lines are guides to the eyes. The magnetic structure in regions I and II is a spin-density wave that is incommensurate with the lattice where region II has a larger magnetic moment on each Ce atom. Region III corresponds to a spin-density wave that is commensurate with the lattice.

mate that approximately $\gamma_0/\gamma \sim 0.12$ (12%) of the Fermi surface remains ungapped below T_N for $CeRhIn_5$ while for Ce_2RhIn_8 92% of the Fermi surface remains ungapped. The results on $CeIn_3$ of Berton *et al.* are also shown in Table I for comparison where $\gamma_0/\gamma \sim 0.94$ (94%). Clearly, the electronic structure, as evidenced by the ratio γ_0/γ, becomes more 3D in the Ce_nRhIn_{2n+3} series as n is increased.[16]

Figure 2 shows the heat capacity in applied magnetic fields for $B||c$ for both compounds ($CeRhIn_5$ on the top and Ce_2RhIn_8 on the bottom). As the magnetic moments are known to lie within the a-plane $CeRhIn_5$, the magnetic field is perpendicular to the magnetic moments in the ordered state in this orientation. The applied field is not sufficient to cause a field-induced magnetic transition in either compound. Rather, it is found that T_N and γ_0 decrease as B is increased as is usually observed in heavy fermion systems.[5]

Figure 3 shows the heat capacity in applied magnetic fields for $B||a$. For both samples, the Neél point (the onset of antiferromagnetic order), and magnetic field-induced transitions of both first and second order are clearly observed. The complete phase diagrams for both $CeRhIn_5$ and Ce_2RhIn_8 showing the various observed transitions are plotted in Fig. 4. The open symbols correspond to second-order transitions (T_N, T_2, and T_1 for Ce_2RhIn_8) and the solid symbols represent the first-order transition (T_1 for $CeRhIn_5$).[17] The dashed lines are merely guides for the eyes. Remarkably, the phase diagrams for both $CeRhIn_5$ and Ce_2RhIn_8 are extremely similar. Region I corresponds to the standard modulated spin-density wave that is incommensurate with the lattice as reported previously in $CeRhIn_5$.[10] The nature of the first- and second-order transitions going from region I to regions II and III is not known, and work is underway to determine the magnetic structures in regions II and III. For Ce_2RhIn_8, region II terminates at 70 kOe while for $CeRhIn_5$ it extends beyond the highest measured field of 90 kOe. The first-order transition going from region I or region II to region III is the same hysteretic field-induced transition observed in magnetization measurements on $CeRhIn_5$ where an increase in the magnetization of $\lesssim 0.006\mu_B$/Ce.[4] These results clearly show that Ce_2RhIn_8 has some 2D electronic and magnetic character.

III. CONCLUSION

In summary, we have measured the anisotropic heat capacity in applied magnetic fields in the quasi-2D heavy-fermion antiferromagnets $CeRhIn_5$ and Ce_2RhIn_8. The magnetic and electronic properties of $CeRhIn_5$ can be well explained by the formation of an anisotropic SDW, leading to a 2D electronic and magnetic structure. The phase diagram of magnetic field-induced magnetic transitions is remarkably

similar for both systems as both a first- and second-order transition are observed in both compounds when the magnetic field is along the tetragonal *a* axis. From the heat capacity measurements, we estimate that $\sim 12\%(\sim 92\%)$ of the Fermi surface remains ungapped below the magnetic ordering temperature for $CeRhIn_5$ (Ce_2RhIn_8). The 2D nature of the electronic properties is a result of the tetragonal crystal structure of Ce_nRhIn_{2n+3} which consists of n cubic ($CeIn_3$) blocks which are weakly interacting along the *c* axis through a ($RhIn_2$) layer. Not surprisingly, it appears that the case of $n=1$ ($CeRhIn_5$) is more anisotropic than the double-layered Ce_2RhIn_8 where the amount of ungapped Fermi surface below T_N is greater than 90%, as is found for the 3D system ($n=\infty$) $CeIn_3$. The similarity of the field-induced transitions in both $CeRhIn_5$ and Ce_2RhIn_8 clearly shows that there is still some 2D character to the magnetic properties of Ce_2RhIn_8. The results here shed light on the unusual magnetic and electronic structure of $CeRhIn_5$ and Ce_2RhIn_8.

Work at UNLV was supported by DOE/EPSCoR Contract No. DE-FG02-00ER45835. Work at LANL was performed under the auspices of the U.S. Department of Energy.

[1] H. Hegger, C. Petrovic, E.B. Moshopoulou, M.F. Hundley, J.L. Sarrao, Z. Fisk, and J.D. Thompson, Phys. Rev. Lett. **84**, 4986 (2000).

[2] J. D. Thompson, R. Movshovich, Z. Fisk, F. Bouquet, N. J. Curro, R. A. Fisher, P. C. Hammel, H. Hegger, M. F. Hundley, M. Jaime, P. G. Pagliuso, C. Petrovic, N. E. Phillips, and J. L. Sarrao, J. Magn. Magn. Mater. (to be published).

[3] While the data are consistent with three crystal-field doublets, it is not sufficient to definitively state the crystal-field levels. Additional measurements are in progress to confirm these findings.

[4] A.L. Cornelius, A.J. Arko, J.L. Sarrao, M.F. Hundley, and Z. Fisk, Phys. Rev. B **62**, 14 181 (2000).

[5] G.R. Stewart, Rev. Mod. Phys. **56**, 755 (1984).

[6] P.C. Canfield and Z. Fisk, Philos. Mag. B **65**, 1117 (1992).

[7] Y.N. Grin, Y.P. Yarmolyuk, and E.I. Gladyshevskii, Sov. Phys. Crystallogr. **24**, 137 (1979).

[8] Y.N. Grin, P. Rogl, and K. Hiebl, J. Less-Common Met. **121**, 497 (1986).

[9] J.M. Lawrence and S.M. Shapiro, Phys. Rev. B **22**, 4379 (1980).

[10] W. Bao, P.G. Pagliuso, J.L. Sarrao, J.D. Thompson, Z. Fisk, J.W. Lynn, and R.W. Erwin, Phys. Rev. B **62**, R14 621 (2000).

[11] W. Bao, P.G. Pagliuso, J.L. Sarrao, J.D. Thompson, Z. Fisk, and J.W. Lynn, Phys. Rev. B **64**, 020401(R) (2001).

[12] C.D. Bredl, J. Magn. Magn. Mater. **63 & 64**, 355 (1987).

[13] N.H. van Dijk, F. Bourdarot, J.P. Klaasse, I.H. Hagmusa, E. Bruck, and A.A. Menovsky, Phys. Rev. B **56**, 14 493 (1997).

[14] S. Murayama, C. Sekine, A. Yokoyanagi, and Y. Onuki, Phys. Rev. B **56**, 11 092 (1997).

[15] V. I. Sidorov (unpublished).

[16] A. Berton, J. Chaussy, G. Chouteau, B. Cornut, J. Flouquet, J. Odin, J. Palleau, J. Peyrard, and R. Tournier, J. Phys. (Paris), Colloq. **40**, C5-325 (1979).

[17] The software used to measure the heat capacity uses average values to fit the thermal relaxation data. From the raw traces, the transitions which we have assigned as first order are clearly first order in nature. Experience tells us that the averaging method underestimates the value of the heat capacity near the peak of the first-order transition by a factor of 4 or 5.